

Dual anchoring strategy to construct ultra-low metal loading

Co/BEA catalyst for propane dehydrogenation

Yulai Lin,^{abcd} Jun Liang,^{abcd} Zijun Huang,^{abcd} Jiaming Dong,^{abcd} Yongming Luo,^{* abcd} and Dedong He ^{* abcd}

^aFaculty of Chemical Engineering, Kunming University of Science and Technology, Kunming 650500, PR China. E-mail: luoyongming@kust.edu.cn, dedong.he@qq.com

^bKey Laboratory of Yunnan Province for Synthesizing Sulfur-containing Fine Chemicals of Yunnan Province, Kunming 650500, PR China

^cThe Innovation Team for Volatile Organic Compounds Pollutants Control and Resource Utilization of Yunnan Province, Kunming 650500, PR China

^dThe Higher Educational Key Laboratory for Odorous Volatile Organic Compounds Pollutants Control of Yunnan Province, Kunming 650500, PR China

Supporting Information

Catalyst characterization.

X-ray diffraction (XRD) patterns of Al β , DeAl β , xCo/ β -SC and xCo/ β -IM samples were recorded on a Rigaku D/MAXRB XRD instrument (Japan) using Cu K α radiation. H₂-Temperature Programmed Reduction (H₂-TPR) experiments were performed using BSD-C200 Automatic Chemisorption Analyzer. 0.05g catalyst was heated in a 100% Ar (30 mL/min) at a ramp rate of 10 °C/min to 700 °C, and the H₂ signal was tracked using a thermal conductivity detector (TCD).

Transmission electron microscopy (TEM) and high-angle annular dark-field scanning TEM (HAADF-STEM) images, along with energy dispersive X-ray spectroscopy mapping, were obtained using a JEOL JEM-F200 instrument operating at 300 kV. iDPC imaging were performed on a were collected on a Thermofisher Spectra 300 at 300 kV. In order to limit the damage of the electron beam, a fast image recording scheme is adopted, using the electron beam current of 1-2 pm.

X-ray photoelectron spectra (XPS) of catalyst samples were carried out on a PHI 5000 Versa Probe II spectrometer equipped with an Al K α X-ray source (1486.6 eV).

The UV-Vis spectra were recorded on a TU-1901 spectrophotometer, and BaSO₄ was

used as the standard for solid samples.

Pyridine adsorption FT-IR was recorded using Bruker VERTEX 70 spectrometer. Specific procedures were as follows: (1) The supporting wafer ($10\text{-}12 \text{ mg/cm}^2$) of sample was pre-treated in the *in-situ* IR cell equipped with CaF_2 window at 400°C for 1 h under high vacuum, then cooled down to 150°C and recorded background spectra between 4000 and 1200 cm^{-1} with 4 cm^{-1} spectral resolution and 32 scans. (2) The activated wafer was exposed to pyridine vapor at 150°C for 0.5 h to obtain saturation adsorption and then the FTIR spectra were scanned after degassed at 150°C for 1 h. Temperature programmed surface reaction (TPSR) measurements of sample are analyzed using an on-line gas chromatograph, equipped with Flame Ionization Detector (FID) and Thermal Conductivity Detector (TCD). Before measurement, the fresh sample (200 mg, 60-100 mesh) is pretreated in pure N_2 ($20 \text{ mL}\cdot\text{min}^{-1}$) at 873 K for 1 h. After cooling down, the measured sample is heated from 373 to 923 K with a step of 3 K min^{-1} in 66 mL min^{-1} of 12% propane flow. The FID and TCD signals of CH_4 , C_2H_6 , C_3H_6 and H_2 are tracked every 3 min.

C_3H_8 FT-IR spectra were recorded using a BRUKER VERTEX 70 spectrometer equipped with a high-temperature reaction chamber. *In-situ* FT-IR spectra with the C_3H_8 consisted of the following steps: (1) The catalyst was pretreated in pure N_2 at 600°C for 30 min, then collected the target temperature background data. (2) 5% $\text{C}_3\text{H}_8/\text{N}_2$ was introduced into the cell. (3) The cell was heated to the desired temperature at a ramp rate of $10^\circ\text{C}/\text{min}$, and FT-IR spectra were acquired at specific temperatures.

Raman spectroscopy is performed by Thermo Fischer DXR Raman Spectrometer with 532 nm laser to analyze the generated coke deposition.

Thermogravimetric-differential thermal analysis (TG-DTA). TG-DTA was measured on a STA449F3 Jupiter instrument. The variation in the weight of spent sample (20 mg) was monitored by increasing the temperature in air ($50 \text{ mL}\cdot\text{min}^{-1}$) from R.T. to 800°C with a heating rate of $10^\circ\text{C}\cdot\text{min}^{-1}$.

Supplementary Figures and Tables

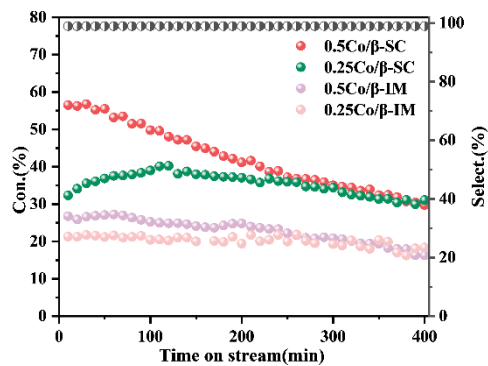


Figure. S1. xCo/β-IM catalytic activity, reaction condition:600°C, m_{cat}:0.2g, 12% C₃H₈ in Ar.

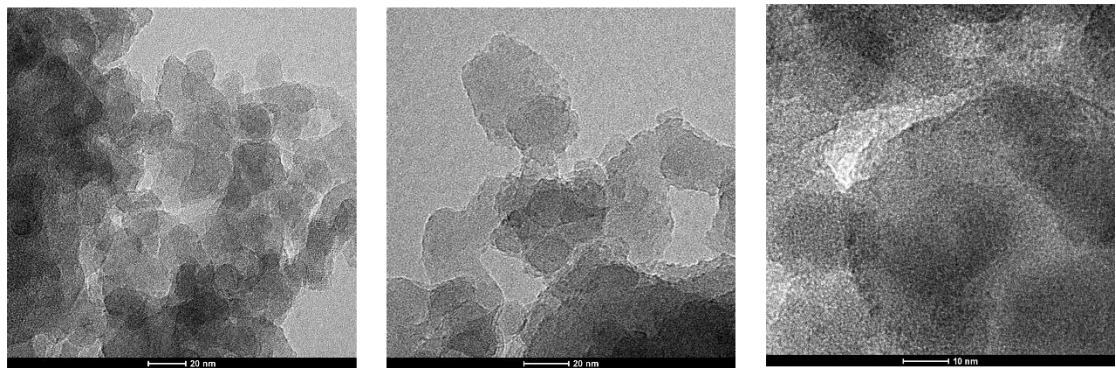


Figure. S2. TEM images of 0.25Co/β-SC

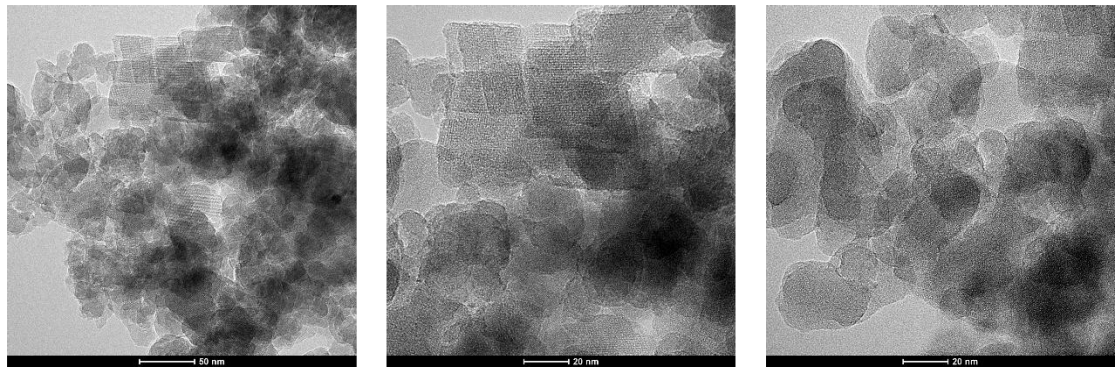


Figure. S3 TEM images of 0.5Co/β-SC

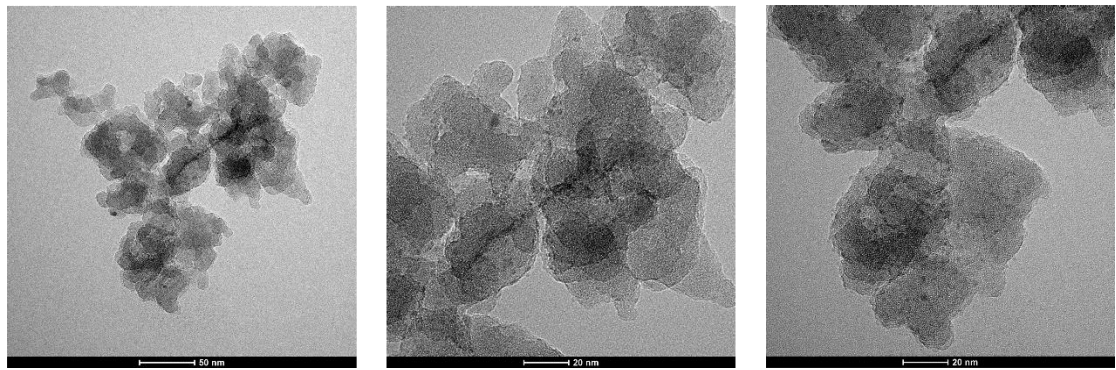


Figure. S4 TEM images of 1.0Co/β-SC

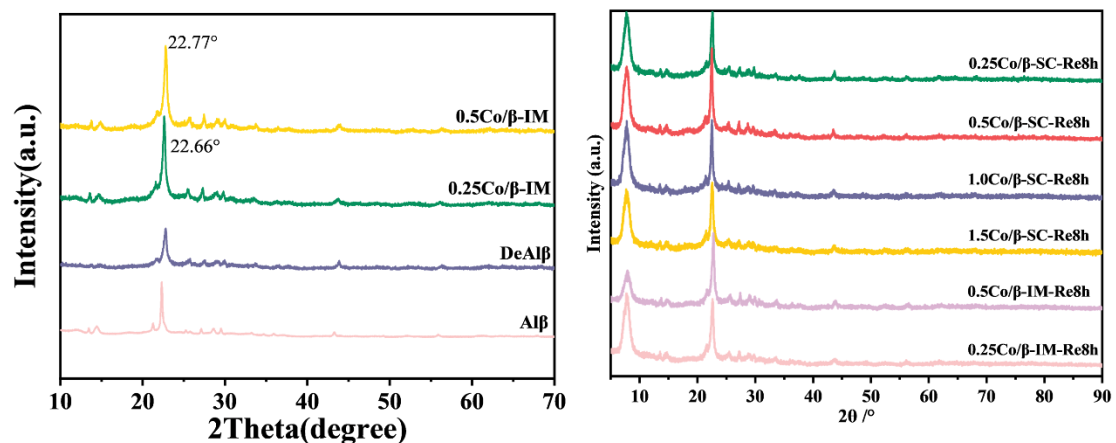


Figure. S5. XRD of $\text{xCo}/\beta\text{-IM}$ (a) and spent catalysts (b)

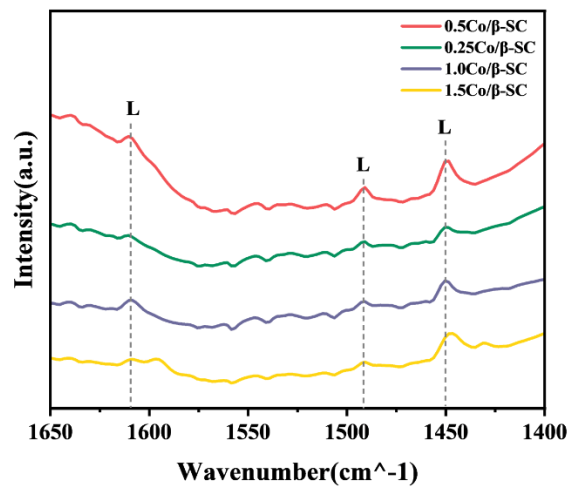


Figure. S6. FT-IR spectra of pyridine adsorption on the different catalysts, desorption at 150 °C

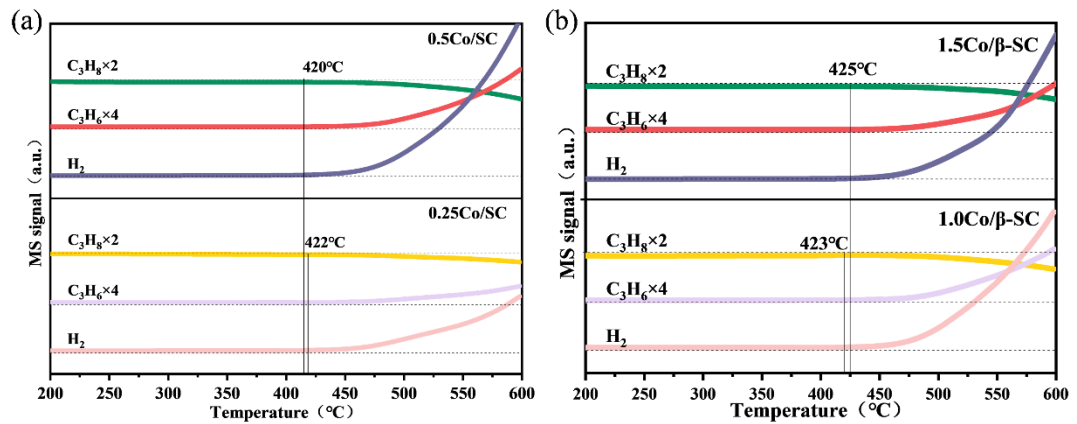


Figure. S7. Propane TPSR and MASS signal of production of 0.25/0.5Co/β-SC(a), 1.0/1.5Co/β-SC(b)

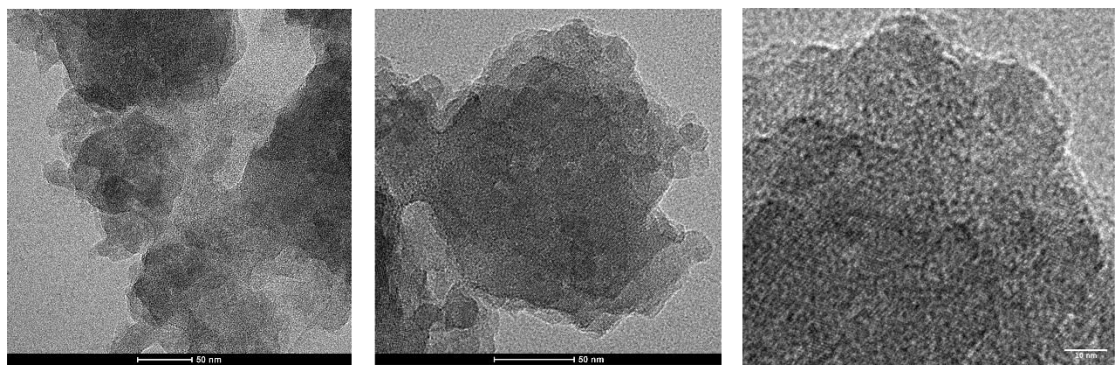


Figure. S8. TEM images of spent 0.25Co/β-SC after 110h PDH

Table S1. Summary of PDH performance data for reported Co containing catalysts.

| Samples | Co loading [wt%] | M cat [g] | T[°C] | C ₃ H ₈ Feed [L·h ⁻¹] | C ₃ H ₈ concentration | Con[%] | Sel[%] | TOF[h ⁻¹] | C ₃ H ₆ formation rate mol _{C₃H₆} [g _{Co} ⁻¹ ·h ⁻¹] | Specific activity [μmol(C ₃ H ₈)g _{Co} ⁻¹ s ⁻¹)] | k _f [mol _{C₃H₆} /g _{Co} ⁻¹ h ⁻¹ bar ⁻¹] | Ref. |
|---|------------------|-----------|-------|---|---|--------|--------|-----------------------|--|---|--|-----------|
| 0.25Co/β-IM | 0.19 | 0.2 | 600 | 0.475 | 12.00% | 20.4 | 99.0 | 670.80 | 667.44 | 3163.53 | 588.69 | This work |
| 0.5Co/β-IM | 0.379 | 0.2 | | | 12.00% | 27.2 | | 448.38 | 446.14 | 2114.59 | 324.91 | |
| 0.25Co/β-SC | 0.145 | 0.2 | | | 12.00% | 40.1 | | 1727.79 | 1719.15 | 8148.40 | 1056.78 | |
| 0.5CO/β-SC | 0.356 | 0.2 | | | 12.00% | 56.7 | | 995.05 | 990.08 | 4692.77 | 638.74 | |
| 1.0Co/β-SC | 0.789 | 0.2 | | | 12.00% | 52.2 | | 413.34 | 411.27 | 1949.35 | 254.34 | |
| 1.5Co/β-SC | 1.431 | 0.2 | | | 12.00% | 52.0 | | 227.03 | 225.89 | 1070.68 | 139.51 | |
| 0.25Co/β-SC | 0.145 | 0.2 | 550 | 0.12 | 10.00% | 42.6 | 99.5 | 463.51 | 461.19 | 2185.96 | 371.27 | |
| Co-m-Al ₂ O ₃ | 1.00 | 0.5 | 600 | 0.600 | 58.80% | 34.0 | 95.0 | 107.24 | 101.88 | 505.75 | 15.65 | 1 |
| Co/γ-Al ₂ O ₃ | 1.10 | 0.5 | 600 | 0.600 | 58.80% | 49.0 | 85.0 | 140.50 | 119.43 | 662.61 | 23.79 | 1 |
| 5Si-5Co-Al ₂ O ₃ | 5.00 | 0.15 | 590 | 1.620 | 20.00% | 25.3 | 91.0 | 143.69 | 130.76 | 677.68 | 66.22 | 2 |
| Co-SBA15 | 2.00 | 0.4 | 600 | 0.300 | 14.29% | 37.0 | 96.0 | 36.48 | 35.02 | 172.06 | 19.29 | 3 |
| Co/γ-Al ₂ O ₃ -NS | 5.00 | 0.3 | 600 | 0.164 | 9.09% | 32.0 | 82.0 | 9.18 | 7.53 | 43.29 | 8.00 | 4 |
| Co/γ-Al ₂ O ₃ -NF | 5.00 | 0.3 | 600 | 0.164 | 9.09% | 30.0 | 70.0 | 8.61 | 6.02 | 40.58 | 7.76 | 4 |
| Co/γ-Al ₂ O ₃ -NP | 5.00 | 0.3 | 600 | 0.164 | 9.09% | 26.0 | 67.0 | 7.46 | 5.00 | 35.17 | 7.31 | 4 |
| Co-Al | 11.10 | 0.2 | 600 | 0.060 | 5.00% | 34.0 | 81.0 | 2.42 | 1.96 | 11.40 | 3.69 | 5 |
| Co-mSiO ₂ | 2.00 | 0.5 | 600 | 0.180 | 10.00% | 36.0 | 71.0 | 17.04 | 12.10 | 80.36 | 12.85 | 6 |
| Co-Zr/SiO ₂ | 1.50 | 0.5 | 550 | 0.036 | 3.00% | 9.5 | 97.0 | 1.20 | 1.16 | 5.65 | 7.90 | 7 |
| Co-Al ₂ O ₃ -HAT | 5.00 | 0.15 | 590 | 0.240 | 20.00% | 24.8 | 97.0 | 20.87 | 20.24 | 98.41 | 9.73 | 8 |
| Co/γ-Al ₂ O ₃ | 5.00 | 3 | 560 | 0.715 | 99.30% | 25.0 | 80.0 | 3.13 | 2.51 | 14.78 | 0.32 | 9 |
| CoO _x @MFI | 1.00 | 0.2 | 600 | 0.120 | 10.00% | 58.0 | 93.0 | 91.51 | 85.10 | 431.55 | 96.25 | 10 |
| CoO/AlO | 3.00 | 0.3 | 600 | 0.480 | 40.00% | 40.0 | 95.0 | 56.10 | 53.29 | 264.55 | 11.30 | 11 |
| Co-MFI | 1.00 | 0.2 | 580 | 0.036 | 5.00% | 38.0 | 96.0 | 17.99 | 17.27 | 84.82 | 26.51 | 12 |
| Co@MFI | 6.00 | 0.3 | 600 | 0.180 | 20.00% | 60.0 | 95.0 | 15.78 | 14.99 | 74.40 | 7.03 | 13 |
| Co@MFI-B50 | 3.00 | 0.1 | 600 | 0.600 | 100.00% | 35.0 | 92.0 | 184.06 | 169.34 | 868.06 | 17.53 | 14 |
| Co-m-Al ₂ O ₃ | 1.00 | 0.5 | 600 | 0.592 | 58.00% | 43.0 | 95.0 | 133.78 | 127.09 | 630.92 | 20.38 | 1 |
| Zn ₁ Co ₁ /NC | 1.00 | 0.1 | 600 | 0.090 | 5.00% | 20.0 | 95.0 | 47.33 | 44.95 | 223.21 | 100.74 | 15 |
| Co@Mo-S-1 | 1.40 | 0.3 | 600 | 0.750 | 25.00% | 40.0 | 95.0 | 187.82 | 178.43 | 885.77 | 57.55 | 16 |
| 5Co1.6Fe/Al ₂ O ₃ | 6.60 | 0.1 | 590 | 0.300 | 20.00% | 22.0 | 95.0 | 26.29 | 24.98 | 124.01 | 13.25 | 17 |
| Co-Zr/SiO ₂ | 7.50 | 0.5 | 550 | 0.036 | 3.00% | 9.0 | 97.0 | 0.23 | 0.22 | 1.07 | 1.57 | 7 |

Table S2. Summary of PDH performance data for reported noble& non- noble metals containing catalysts.

| Samples | M loading [wt%] | M cat [g] | T[°C] | C ₃ H ₈ Feed [L·h ⁻¹] | C ₃ H ₈ concentration | Con[%] | Sel[%] | TOF[h ⁻¹] | C ₃ H ₆ formation rate mol _{C₃H₆} [g _{Co} ⁻¹ ·h ⁻¹] | Specific activity [μmol(C ₃ H ₈)g _M ⁻¹ S ⁻¹] | k _f [mol _{C₃H₆} /g _M ⁻¹ h ⁻¹ bar ⁻¹] | Ref. |
|---|-----------------|-----------|-------|---|---|--------|--------|-----------------------|--|---|---|------|
| PtLa/mz-deGa | 1.00 | 0.05 | 580 | 0.280 | 100.00% | 40.0 | 98.0 | 1952.19 | 1913.15 | 2779.76 | 84.90 | 18 |
| PtSn/2Mg-SBA-15 | 1.00 | 0.2 | 580 | 0.840 | 70.00% | 35.7 | 95.0 | 1305.82 | 1240.53 | 1859.38 | 49.55 | 19 |
| PtGa-R | 0.50 | 0.2 | 600 | 0.600 | 10.00% | 40.0 | 95.0 | 2090.14 | 1985.64 | 2976.19 | 460.52 | 20 |
| PtZnAl _{0.2} /SBA-15 | 0.50 | 0.2 | 590 | 0.253 | 16.67% | 55.9 | 99.0 | 1233.14 | 1220.81 | 1755.89 | 177.97 | 21 |
| Pt-Sn/CeO ₂ | 1.00 | 0.1 | 580 | 0.120 | 3.85% | 39.5 | 84.5 | 412.80 | 348.82 | 587.80 | 232.88 | 22 |
| Pt-Sn/Al ₂ O ₃ | 1.00 | 0.1 | 580 | 0.120 | 3.85% | 32.6 | 71.4 | 340.69 | 243.26 | 485.12 | 208.10 | 22 |
| Pt/Zn-Al ₂ O ₃ | 0.85 | 0.1 | 600 | 0.252 | 14.00% | 46.0 | 97.0 | 1187.69 | 1152.06 | 1691.18 | 186.83 | 23 |
| Pt-Zn ₃ O _x @RUB-15 | 0.50 | 1 | 600 | 0.594 | 33.00% | 40.0 | 96.0 | 413.85 | 397.29 | 589.29 | 29.79 | 24 |
| Rh(0.5)Sn(3.0) | 0.50% | 0.1 | 600 | 0.400 | 33.30% | 30.0 | 96.0 | 1102.39 | 1058.29 | 2975.89 | 160.98 | 25 |
| NiV ₂ O ₃ /Al ₂ O ₃ | 3.00 | 0.5 | 500 | 0.216 | 16.67% | 16.5 | 95.1 | 6.23 | 5.92 | 29.46 | 4.65 | 26 |
| 0.5NiSiBeta | 0.50 | 0.3 | 600 | 0.075 | 6.25% | 35.0 | 84.0 | 45.85 | 38.52 | 217.01 | 55.70 | 27 |
| Ni/Al ₂ O ₃ | 1.00 | 0.5 | 580 | 0.240 | 20.00% | 29.4 | 93.0 | 36.97 | 34.39 | 175.00 | 15.92 | 28 |
| 0.2Ni0.06Zn-S-1 | 0.20 | 0.32 | 600 | 0.300 | 23.26% | 20.0 | 90.0 | 245.62 | 221.06 | 1162.53 | 114.00 | 29 |
| (1:1 Ni:Ga) @Ni ₃ Ga/Al ₂ O ₃ | 5.00 | 0.1 | 600 | 0.120 | 10.00% | 13.0 | 94.0 | 8.17 | 7.68 | 38.69 | 12.34 | 30 |
| (3Fe:P)/Al ₂ O ₃ | 13.30 | 0.14 | 600 | 0.030 | 5.00% | 12.0 | 82.4 | 0.48 | 0.40 | 2.40 | 1.64 | 31 |
| (2Fe:P)/Al ₂ O ₃ | 3.00 | 0.2 | 600 | 0.600 | 5.00% | 35.0 | 92.0 | 0.34 | 0.28 | 1.68 | 1.15 | 31 |
| (1Fe:P)/Al ₂ O ₃ | 1.00 | 0.4 | 600 | 0.592 | 5.00% | 43.0 | 95.0 | 0.17 | 0.14 | 0.84 | 0.57 | 31 |
| 20Fe/5S-Al | 20.00 | 2 | 560 | 0.009 | 1.20% | 20.0 | 80.0 | 0.01 | 0.01 | 0.05 | 0.10 | 32 |
| Cr-MSU-x28 | 1.27 | 0.2 | 600 | 0.180 | 10.00% | 30.0 | 90.0 | 49.35 | 44.42 | 263.64 | 45.87 | 33 |
| Cr/HZSM-5(260) | 5.00 | 0.2 | 580 | 0.060 | 5.00% | 32.6 | 94.2 | 4.54 | 4.28 | 24.26 | 8.07 | 34 |
| Mo-SH | 5.00 | 0.5 | 600 | 0.120 | 10.00% | 37.0 | 92.0 | 7.61 | 7.00 | 22.02 | 3.49 | 35 |
| | | | 550 | | | 20.0 | 86.0 | 4.11 | 3.54 | 11.90 | 2.74 | 35 |
| 12V/Al | 12.00 | 0.25 | 600 | 0.420 | 28.00% | 32.0 | 94.0 | 10.19 | 9.58 | 55.56 | 3.45 | 36 |
| 1VZr | 1.00 | 0.4 | 550 | 0.420 | 14.00% | 25.0 | 90.0 | 59.70 | 53.73 | 325.52 | 46.95 | 37 |
| PV-0.7 | 10.00 | 1 | 610 | 0.360 | 20.00% | 50.0 | 88.5 | 4.09 | 3.62 | 22.32 | 1.77 | 38 |
| ZnO-S-1_3 | 1.20 | 0.05 | 550 | 0.960 | 40.00% | 31.0 | 87.0 | 1447.70 | 1259.50 | 6150.79 | 338.15 | 39 |
| | | | 600 | | | 40.0 | 88.0 | 1868.00 | 1643.84 | 7936.51 | 339.14 | 39 |

| | | | | | | | | | | | | |
|---------|------|------|-----|-------|--------|------|------|-------|-------|--------|------|----|
| ZnO@S-1 | 4.00 | 0.15 | 600 | 0.362 | 67.00% | 31.4 | 93.9 | 55.26 | 51.89 | 234.80 | 6.58 | 40 |
|---------|------|------|-----|-------|--------|------|------|-------|-------|--------|------|----|

Supplementary References

1. F. Ebert, P. Ingale, S. Vogl, S. Praetz, C. Schlesiger, N. Pfister, R. N. d'Alnoncourt, B. R. Cuenya, A. Thomas, E. Gioria and F. Rosowski, *Acs Catalysis*, 2024, **14**, 9993-10008.
2. Y. H. Dai, Y. Wu, H. Dai, X. Gao, S. Y. Tian, J. J. Gu, X. F. Yi, A. M. Zheng and Y. H. Yang, *Journal of Catalysis*, 2021, **395**, 105-116.
3. Z. J. Huang, D. D. He, W. H. Deng, G. W. Jin, K. Li and Y. M. Luo, *Nat Commun*, 2023, **14**.
4. N. Dewangan, J. Ashok, M. Sethia, S. Das, S. Pati, H. Kus and S. Kawi, *Chemcatchem*, 2019, **11**, 4923-4934.
5. B. Hu, W. G. Kim, T. P. Sulmonetti, M. L. Sarazen, S. Tan, J. So, Y. J. Liu, R. S. Dixit, S. Nair and C. W. Jones, *Chemcatchem*, 2017, **9**, 3330-3337.
6. Z. F. Bian, N. Dewangan, Z. G. Wang, S. Pati, S. B. Xi, A. Borgna, H. Kus and S. Kawi, *Acs Applied Nano Materials*, 2021, **4**, 1112-1125.
7. Y. Q. Zhao, H. Sohn, B. Hu, J. Niklas, O. G. Poluektov, J. Tian, M. Delferro and A. S. Hock, *Acs Omega*, 2018, **3**, 11117-11127.
8. Y. H. Dai, J. J. Gu, S. Y. Tian, Y. Wu, J. C. Chen, F. X. Li, Y. H. Du, L. M. Peng, W. P. Ding and Y. H. Yang, *Journal of Catalysis*, 2020, **381**, 482-492.
9. Y. N. Sun, Y. M. Wu, H. H. Shan and C. Y. Li, *Catalysis Letters*, 2015, **145**, 1413-1419.
10. J. L. Liu, J. N. Wang, Y. N. Zhang, W. Zheng, Y. B. Yao, Q. Liu, X. J. Zhang, Y. A. Yang and X. Wang, *Acs Catalysis*, 2023, **13**, 14737-14745.
11. Q. Shi, Y. Y. Song, D. Li, Y. Wang, Z. Xie, X. Q. Fan, L. Kong, X. Xiao and Z. Zhao, *Journal of Catalysis*, 2024, **433**.
12. Z. P. Hu, G. Qin, J. Han, W. Zhang, N. Wang, Y. Zheng, Q. Jiang, T. Ji, Z. Y. Yuan, J. Xiao, Y. Wei and Z. Liu, *J Am Chem Soc*, 2022, **144**, 12127-12137.
13. Y. Xu, W. Hu, Y. Li, H. Su, W. Liang, B. Liu, J. Gong, Z. Liu and X. Liu, *ACS Catalysis*, 2023, **13**, 1830-1847.
14. X. Lv, M. Yang, S. Song, M. Xia, J. Li, Y. Wei, C. Xu, W. Song and J. Liu, *ACS Appl Mater Interfaces*, 2023, DOI: 10.1021/acsami.2c21076.
15. Y. C. Chai, S. H. Chen, Y. Chen, F. F. Wei, L. R. Cao, J. Lin, L. Li, X. Y. Liu, S. Lin, X. D. Wang and T. Zhang, *Journal of the American Chemical Society*, 2023, **146**, 263-273.
16. Z. Q. Qu, G. Y. He, T. J. Zhang, Y. Q. Fan, Y. X. Guo, M. Hu, J. Xu, Y. H. Ma, J. C. Zhang, W. B. Fan, Q. M. Sun, D. H. Mei and J. H. Yu, *Journal of the American Chemical Society*, 2024, **146**, 8939-8948.
17. C. W. Zhang, J. Wen, L. Wang, X. G. Wang and L. Shi, *New J Chem*, 2020, **44**, 7450-7459.
18. R. Ryoo, J. Kim, C. Jo, S. W. Han, J. C. Kim, H. Park, J. Han, H. S. Shin and J. W. Shin, *Nature*, 2020, **585**, 221-+.
19. B. Li, Z. X. Xu, F. L. Jing, S. Z. Luo and W. Chu, *Appl Catal a-Gen*, 2017, **533**, 17-27.
20. Y. Xu, J. N. Chen, X. L. Yuan, Y. Zhang, J. Q. Yu, H. Y. Liu, M. H. Cao, X. Fan, H. P. Lin and Q. Zhang, *Ind Eng Chem Res*, 2018, **57**, 13087-13093.
21. X. Q. Fan, J. M. Li, Z. Zhao, Y. C. Wei, J. Liu, A. J. Duan and G. Y. Jiang, *Catal Sci Technol*, 2015, **5**, 339-350.
22. H. F. Xiong, S. Lin, J. Goetze, P. Pletcher, H. Guo, L. Kovarik, K. Artyushkova, B. M.

- Weckhuysen and A. K. Datye, *Angew Chem Int Edit*, 2017, **56**, 8986-8991.
23. Y. N. Xing, B. N. Li, L. L. Kang, Y. Su, X. L. Pan, L. Li, H. Liu, X. Y. Liu, A. Q. Wang and T. Zhang, *J Phys Chem C*, 2024, **129**, 244-252.
24. D. Liu, F. Jiang, Q. Zhang, W. H. Huang, Y. Zheng, M. Chen, L. Wu, R. Qin, M. Wang, S. Zhang, L. Chen, K. Yan, L. Zhou, Y. Zhao, L. Gu and G. Chen, *ACS Nano*, 2024, **18**, 34671-34682.
25. P. Natarajan, H. A. Khan, A. Jaleel, D. S. Park, D. C. Kang, S. Yoon and K. D. Jung, *Journal of Catalysis*, 2020, **392**, 8-20.
26. G. M. Li, B. Wang, X. C. Dai, F. Shi, Y. Ding and X. J. Cui, *Catal Sci Technol*, 2025, **15**, 318-322.
27. X. Zhou, S. J. Wu, Y. M. Luo, L. H. Zhu and D. D. He, *Energy & Fuels*, 2023, **37**, 450-458.
28. R. Ma, J. X. Gao, J. J. Kou, D. P. Dean, C. J. Breckner, K. J. Liang, B. Zhou, J. T. Miller and G. J. Zou, *Acs Catalysis*, 2022, **12**, 12607-12616.
29. C. M. Huang, D. M. Han, L. J. Guan, L. H. Zhu, Y. Mei, D. D. He and Y. Zu, *Fuel*, 2022, **307**.
30. Y. He, Y. J. Song, D. A. Cullen and S. Laursen, *Journal of the American Chemical Society*, 2018, **140**, 14010-14014.
31. S. Tan, B. Hu, W. G. Kim, S. H. Pang, J. S. Moore, Y. J. Liu, R. S. Dixit, J. G. Pendergast, D. S. Sholl, S. Nair and C. W. Jones, *Acs Catalysis*, 2016, **6**, 5673-5683.
32. Y. N. Sun, L. Tao, T. Z. You, C. Y. Li and H. H. Shan, *Chemical Engineering Journal*, 2014, **244**, 145-151.
33. J. Baek, H. J. Yun, D. Yun, Y. Choi and J. Yi, *Acs Catalysis*, 2012, **2**, 1893-1903.
34. Z.-P. Hu, Y. Wang, D. Yang and Z.-Y. Yuan, *Journal of Energy Chemistry*, 2020, **47**, 225-233.
35. M. A. Abedin, S. Kanitkar, S. Bhattar and J. J. Spivey, *Appl Catal a-Gen*, 2020, **602**.
36. G. Liu, Z. J. Zhao, T. F. Wu, L. Zeng and J. L. Gong, *Acs Catalysis*, 2016, **6**, 5207-5214.
37. Y. F. Xie, R. Luo, G. D. Sun, S. Chen, Z. J. Zhao, R. T. Mu and J. L. Gong, *Chem Sci*, 2020, **11**, 3845-3851.
38. Y. Gu, H. J. Liu, M. M. Yang, Z. P. Ma, L. M. Zhao, W. Xing, P. P. Wu, X. M. Liu, E. L. N. Mintova, P. Bai and Z. F. Yan, *Appl Catal B-Environ*, 2020, **274**.
39. D. Zhao, X. N. Tian, D. E. Doronkin, S. L. Han, V. A. Kondratenko, J. D. Grunwaldt, A. Perechodjuk, T. H. Vuong, J. Rabehah, R. Eckelt, U. Rodemerck, D. Linke, G. Y. Jiang, H. J. Jiao and E. V. Kondratenko, *Nature*, 2022, **601**, E8-E8.
40. S. J. Song, K. Yang, P. Zhang, Z. J. Wu, J. Li, H. Su, S. Dai, C. M. Xu, Z. X. Li, J. Liu and W. Y. Song, *Acs Catalysis*, 2022, **12**, 5997-6006.